Data-Driven Reserve Allocation With Frequency Security Constraint Considering Inverter Air Conditioners

XINRAN ZHUANG[1], CHENGJIN YE[1], YI DING[1], HONGXUN HUI[1], AND BO ZOU[2]

[1]College of Electrical Engineering, Zhejiang University, Hangzhou 310000, China
[2]The Economics Research Institute of State Grid Zhejiang Electric Power Company Ltd., Hangzhou 310000, China

Corresponding author: Chengjin Ye (yechenjing@zju.edu.cn)

ABSTRACT Inverter air conditioners (IACs) with considerable total capacity and fast response speed are ideal demand response resources, which are of significant potential to provide reserve capacity for the power system frequency regulation. However, due to the complexity and implicitness of the frequency response models, it is difficult to formulate the optimization problem considering frequency dynamics to allocate reserve capacity precisely. In this paper, a data-driven method is proposed for reserve allocation with the frequency security constraint considering IACs. Firstly, the equivalent frequency response model of aggregated IACs is developed considering electrical-thermal characteristics and then incorporated into the frequency regulation framework of power systems along with conventional generators. Then, simulations are implemented to generate massive reserve samples with deterministic frequency security labels. Later, a support vector machine (SVM) based frequency security classifier is trained to convert the implicit frequency security constraint into polynomials and reshape the reserve allocation problem into a solvable general quadratically constrained quadratic program (QCQP). Finally, a heuristic Suggest-and-Improve (SI) method is adopted to deal with the nonconvex QCQP of interest. It is demonstrated by numerical studies that the proposed data-driven method enables power systems to operate closer to the frequency security boundaries and thus achieve lower costs.

INDEX TERMS Reserve allocation, frequency security constraint, inverter air conditioner, classifier, data-driven.

I. INTRODUCTION

Frequency stabilization is vital for the security and reliability of power system operation. The large frequency deviation may result in generator cascade tripping and is one of the main causes of power system blackout [1]. The power system frequency is directly affected by the power generation and demand [2], which tends to rise when power generation is larger than demand, and fall when the generation is insufficient. Due to the fluctuations of the power supply and demand, the power imbalance cannot be avoided completely in power systems. Therefore, the frequency regulation, including primary frequency regulation (PFR) and secondary frequency regulation (SFR), is widely adopted to maintain the stability of power systems [3].

The associate editor coordinating the review of this article and approving it for publication was Md. Apel Mahmud.

Reserve allocation is one of the main issues in the frequency regulation. The frequency dynamics are seldom considered in previous researches of reserve allocation for PFR and SFR, which focus more on the power balance of the systems [4]. Recently, the power system frequency stability has been greatly threatened by the increasing penetration of renewable energies [5] and more researches have followed the reserve allocation considering the frequency dynamics with interest. Generally, the frequency response model is fundamental to investigate the frequency dynamics. In [6], the PFR and SFR models are formulated based on the swing equations. In [7], an adaptive frequency response model is proposed, which is integrated with the load shedding scheme. In [8], an adaptive multiple-machine frequency response model is presented incorporating the governor response.

Due to the high nonlinearity and complexity of frequency response models, the frequency security constraint associated

with frequency dynamics cannot be incorporated directly in the power system reserve allocation problem. In [9], linearization is performed to simplify the generation frequency dynamics, which is relatively inaccurate. In [10], the sufficient condition for frequency security is proposed as an affine constraint of the unit commitment problem, which is a conservative estimation and may lead to an overestimated reserve requirement. In [11], the piece-wise linearization is utilized to transform the frequency limit into a linear arithmetic equation, whose complexity increases greatly with subject to the number of system components.

Recently, demand side resources have been widely considered to have the potential for power system frequency regulation [12], [13], among which, the inverter air conditioners (IACs) are most concerned. The reasons are as follows: 1) Air conditioning (AC) is one of the top power-consuming appliances [14], and most of the newly installed ACs are IACs [15]; 2) IACs can adjust the input power very quickly [16]. Moreover, short time adjustment of IAC power has little effect on users, relatively [17]. As IACs are considered as an ideal demand response resource, it is significant to consider the IACs in power system frequency regulation. In [18], the IACs are modeled as a thermal battery. In [19], the equivalent frequency response model of IACs has been presented including equivalent transfer functions, control parameters, and evaluation criteria. In [20], the IACs are combined with the conventional generator model for frequency regulation service. However, in these existing studies, the response characteristics of IACs are mainly supported by simulation, which have not been integrated into the reserve allocation optimization problem due to the complexity of the model of IACs.

Machine learning classifier (MLC) is widely utilized [21] due to its attractive model-free advantage, which has been successfully applied in power system studies such as component fault diagnosis, load forecasting, power quality evaluation and so on [22]–[24]. From the perspective of classification, whether the frequency security constraint is satisfied can be considered as a binary problem. Thus, MLC does have the possibility to be applied to deal with the implicitness of power system frequency security constraint, which has not been reported yet.

In this paper, a data-driven method for reserve allocation with frequency security constraint considering IACs has been proposed. Firstly, the equivalent frequency response model of IACs is presented and integrated into the power system model. Then, with the utilization of a machine learning frequency security classifier (MLFSC) based on support vector machine (SVM), the reserve allocation problem between IACs and conventional generators considering frequency security constraint is converted to a general quadratically constrained quadratic program (QCQP) [25]. The general QCQP is solved by the heuristic Suggest-and-Improve (SI) method. The framework of this paper is illustrated in Fig. 1.
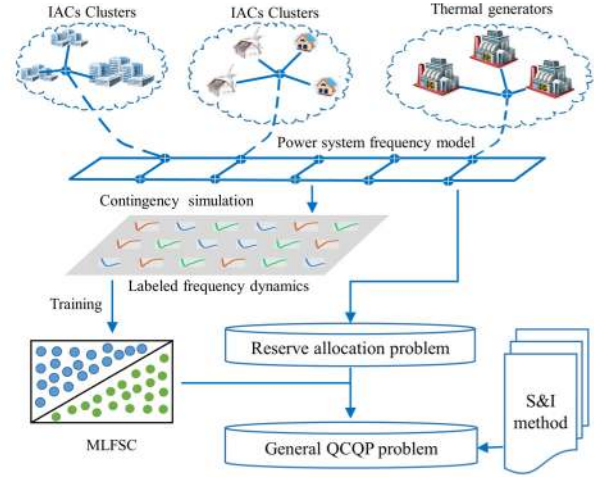

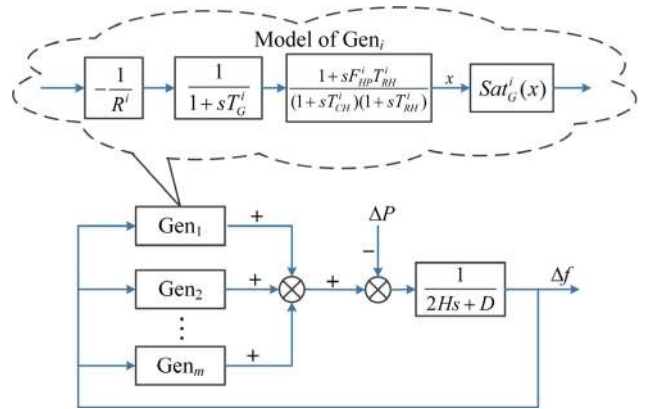**FIGURE 1.** Framework of the proposed data-driven power system reserve allocation.

FIGURE 2. Classical power system frequency response model.

II. MODELLING OF POWER SYSTEM FREQUENCY RESPONSE INTEGRATED WITH IACs

In this section, the model for power system frequency response is introduced firstly. Then, the equivalent frequency response model of IACs is presented. Finally, the aggregated model of IACs is integrated into the power system frequency response framework. Note that all the models in this part are constructed in the frequency domain.

A. POWER SYSTEM FREQUENCY RESPONSE MODEL

The classical frequency response model participated by m conventional generators is illustrated in Fig. 2 [6].

In Fig. 2, the input ΔP is the power imbalance of the power system; the output Δf is the corresponding frequency deviation considering the frequency regulation. H is the equivalent system inertia and D is the load-damping rate. The frequency regulation provided by the conventional generator i is illustrated in the dashed line box. R^i and T_G^i are the governor speed regulation and time constant of generator i, respectively. T_{CH}^i and T_{RH}^i are the steam chest time and reheat turbine time constants of generator i, respectively. F_{HP}^i is the

high-pressure power fraction of reheat turbine of generator i. $Sat_G^i(x)$ is a saturation block representing the reserve capacity R_G^i of generator i. It is defined as:

$$Sat_G^i(x) = \begin{cases} x, & 0 < x < R_G^i \\ R_G^i, & x \geq R_G^i \end{cases} \quad (1)$$

B. EQUIVALENT FREQUENCY RESPONSE MODEL OF IACS

The IACs have large regulation capacity and can be regard as an important resource to maintain the power system frequency stability [20]. The equivalent frequency response model of an IAC can be constructed based on its thermal and electrical models.

The thermal model of an IAC is built based on the modeling of the room temperature deviation [26]:

$$C_{room} V_{room} \rho_A T_{room}(s) = Q_{room}(s) - Q_{AC}(s) \quad (2)$$
$$Q_{room}(s) = H_r [T_{out}(s) - T_{room}(s)] \quad (3)$$

where C_{room} and V_{room} are the room thermal mass and room volume, respectively; ρ_A is the density of the air; Q_{room} and Q_{AC} are the room heat gain and the refrigerating capacity of the IAC, respectively; T_{out} and T_{room} are the outdoor and room temperature, respectively; H_r is the equivalent thermal conductance between the room and the outdoor air.

IACs can adjust the operating frequency in order to control their operating power. And the electrical model of an IAC is constructed based on this feature [17]:

$$P_{AC}(s) = \frac{\theta_P}{T_c s + 1} f_{AC}(s) + P_c \quad (4)$$
$$Q_{AC}(s) = \frac{\theta_Q}{T_c s + 1} f_{AC}(s) + Q_c \quad (5)$$

where θ_P and θ_Q are the control parameters of the IAC; f_{AC} and P_{AC} are the operating frequency and operating power, respectively; T_c is the compressor time constant of the IAC; P_c and Q_c are the baseline operating power and refrigerating capacity, respectively.

The mechanism for an IAC to participate in the power system frequency response is to adjust its operating frequency based on the system frequency deviation, so that its operating power is changed correspondingly. The relationship between the IAC operating frequency and the system frequency can be obtained by [19]:

$$\Delta f_{AC}(s) = A\Delta f(s) + C(s)(\Delta T_{room}(s) - \Delta T_{set}(s)) \quad (6)$$
$$C(s) = \alpha + \frac{\beta}{s} \quad (7)$$

where A is the control coefficient that is analogous to the $1/R$ of generators; $C(s)$ is the temperature controller of IACs, which is a proportional-integral (PI) controller as illustrated in (7); T_{set} is the IAC set temperature. The operating frequency of an IAC is determined jointly by the system frequency and the deviation of room and set temperature.

Based on the thermal and electrical models represented by (1) – (7), the response of the operating power of IACs to the

power system frequency deviation can be obtained by:

$$\Delta P_{AC}(s) = F_1(s) + F_2(s) \quad (8)$$
$$F_1(s) = \frac{\theta_p(C_{room} V_{room} \rho_A s + H_r)(A\Delta f(s) + C(s)\Delta T_{set}(s))}{(T_c s + 1)(C_{room} V_{room} \rho_A s + H_r) + \theta_Q C(s)} \quad (9)$$
$$F_2(s) = \frac{\theta_p C(s)(H_r \Delta T_{out}(s))}{(T_c s + 1)(C_{room} V_{room} \rho_A s + H_r) + \theta_Q C(s)} \quad (10)$$

It can be seen from (8) – (10) that the IAC operating power is affected by the system frequency, the room temperature, and the set temperature. As the primary frequency response is implemented within seconds [6], it is reasonable to assume that the room temperature and set temperature remain constant during this process. Consequently, (8) – (10) can be simplified as follows:

$$\Delta P_{AC}(s) = \frac{\theta_p A(T_a s + 1)\Delta f(s)}{(T_c s + 1)(T_a s + 1) + \Phi_{AC} C(s)} \quad (11)$$
$$T_a = \frac{C_{room} V_{room} \rho_A}{H_r} \quad (12)$$
$$\Phi_{AC} = \frac{\theta_Q}{H_r} \quad (13)$$

It can be seen that (11) – (13) exactly constitute the equivalent frequency response model of a single IAC.

Due to the spreading demand response, more IACs especially the central types for commercial or factory buildings have been participating in the power system operation control. Such IACs are configured with specific control programs and can be connected to the wireless network, so as to be monitored and remotely controlled. The manufacturers accept or proactively promote such programs, and agree to disclose the necessary IAC parameters, by which they can increase the added values and popularity of their products and expand the sales volumes [27], [28]. In some particular cases, the manufacturers directly participate in the demand response projects and share the incomes with the load aggregators. This paper is based on the above scenario, where the IAC manufacturers are associated with the demand response projects and the necessary information about the equipment are available.

C. POWER SYSTEM FREQUENCY RESPONSE MODEL WITH AGGREGATED IACS

The operating power of a single IAC has no significance for a realistic power system. The response of IACs only makes sense with the simultaneous participation of multiple ones. Considering the large quantity of existing IACs (like tens of thousands) and their non-uniform parameters, the clustering method is utilized in this section to avoid the curse of dimensionality.

Specifically, the k-means clustering algorithm [29] is utilized to cluster massive IACs. Assume that the IACs are of different T_c and A. Then the dataset to be clustered is $\{(T_c^1, A^1), (T_c^2, A^2), \cdots, (T_c^d, A^d)\}$ where T_c^i and A^i are the corresponding parameters of IAC i and d is the total IACs

number. $\mathbf{C} = \{(\tilde{T}_c^1, \tilde{A}^1), (\tilde{T}_c^2, \tilde{A}^2), \cdots, (\tilde{T}_c^n, \tilde{A}^n)\}$ is the cluster centers, which can be calculated by:

$$\mathbf{C} = \arg \min \sum_{i=1}^d (T_c^i - T_c^{(i)})^2 + (A^i - A^{(i)})^2$$

$$(T_c^{(i)}, A^{(i)}) = \arg \min_{(T_c^{(j)}, A^{(j)}) \in \mathbf{C}} [(T_c^i - T_c^{(j)})^2 + (A^i - A^{(j)})^2]$$

$$(14)$$

where n is the number of clusters and $(T_c^{(i)}, A^{(i)})$ represents the cluster centroid that (T_c^i, A^i) belongs to.
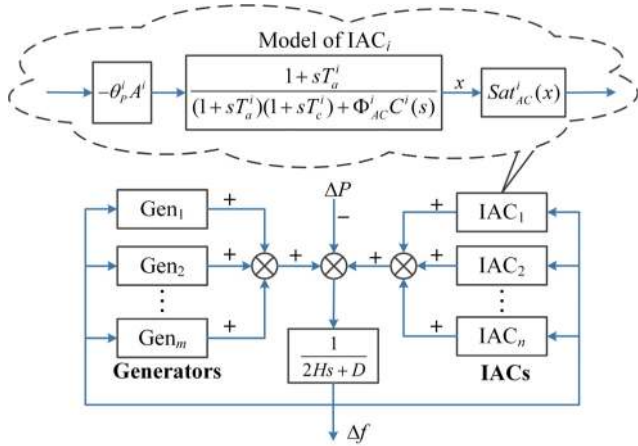

FIGURE 3. Power system frequency response model integrated with IACs and conventional generators.

The IACs are divided into n aggregated ones with the centroid parameters $\mathbf{C}$. Then the power system frequency response model considering the demand response of IACs can be shown in Fig. 3, where the aggregated IAC can be considered as a kind of Virtual Power Plants (VPPs) [30].

III. DATA-DRIVEN RESERVE ALLOCATION WITH FREQUENCY SECURITY CONSTRAINT

A. PROBLEM DESCRIPTION

The main issue of primary frequency regulation is the allocation of power system reserves. Note that the response of IACs is faster than conventional generators due to the smaller time constant [19]. The utilization of IAC reserve can naturally restrain the frequency deviation significantly, while the reserves of IACs are relatively expensive than those of conventional generators in many circumstances. Therefore, the allocation of reserves provided by IACs and generators is indeed an optimization problem, where the frequency security constraint and the overall reserve cost should be considered simultaneously.

The objective of the allocation problem fitting the established frequency regulation framework in Fig. 3 is formulated as follows:

$$\min_{R_G, R_{AC}} C_G^T R_G + C_{AC}^T R_{AC} \qquad (15)$$

where C_G and C_{AC} are the reserve price vectors of generators and aggregated IACs, respectively; R_G and R_{AC} are
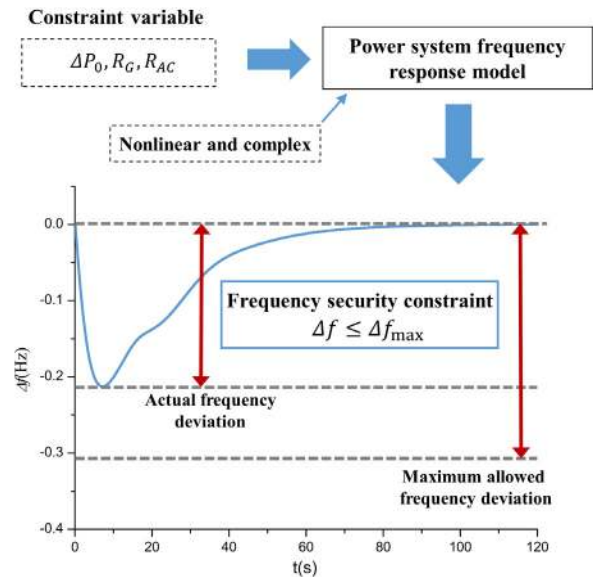

FIGURE 4. Security constraint in terms of the maximum allowed frequency deviation.

the reserve capacity of generators and aggregated IACs, respectively.

The maximum allowed frequency deviation Δf_{max} is utilized to ensure the frequency security as illustrated in Fig. 4. The system reserve allocation scheme should meet the security requirement that the maximum frequency deviation caused by a specific power imbalance ΔP_0 is within the threshold Δf_{max}. Therefore the frequency security constraint can be written as follows:

$$-\min[FR(\Delta P_0, R_G, R_{AC})] \le \Delta f_{max} \qquad (16)$$

where $FR(\cdot)$ is the system frequency response model.

However, the frequency security constraint in (16) is implicit due to the nonlinear and complex frequency response models as illustrated in Fig. 3, which deters it from being integrated into a solvable optimization problem. In order to deal with the difficulty, the MLFSC is utilized in next section to reconstruct the frequency security constraint in a data-driven way.

In addition, the allowed range of the reserve capacity of generators and IACs, as well as the system power flow, should be considered in the reserve allocation problem:

$$R_G^{min} \le R_G \le R_G^{max} \qquad (17)$$

$$R_{AC}^{min} \le R_{AC} \le R_{AC}^{max} \qquad (18)$$

$$\left| T \cdot A \begin{bmatrix} R_G \\ R_{AC} \end{bmatrix} \right| \le F_{max} \qquad (19)$$

where R_G^{min} and R_G^{max} are the minimum and maximum allowed reserves of generators, respectively; R_{AC}^{min} and R_{AC}^{max} are the minimum and maximum allowed reserves of IACs, respectively; T is the power transmission distribution factor (PTDF) and A is the adjacency matrix; F_{max} is the power flow threshold.

B. DATA-DRIVEN APPROXIMATION OF FREQUENCY SECURITY CONSTRAINT

In this paper, the MLFSC is trained to judge whether the system frequency deviation violates the $\Delta f_{\max}$. Firstly, the feature vector x for the MLFSC is:

$$x = (\Delta P, R_G^1, R_G^2, \cdots, R_G^m, R_{AC}^1, R_{AC}^2, \cdots, R_{AC}^n) \quad (20)$$

where R_G^i and R_{AC}^j are the reserve capacities of generator i and aggregated IAC j, respectively; m and n are the numbers of generators and aggregated IACs, respectively. The training dataset $\{\mathbf{x}, \mathbf{y}\}$ is composed of multiple feature vectors along with their labels:

$$\mathbf{x} = \{x_1, x_2, \cdots, x_k\} \quad (21)$$

$$\mathbf{y} = \{y_1, y_2, \cdots, y_k\} \quad (22)$$

$$y_i = \begin{cases} 1, & -\min(FR(x_i)) > \Delta f_{\max} \\ -1, & -\min(FR(x_i)) \le \Delta f_{\max} \end{cases} \quad (23)$$

As illustrated in Fig. 5, the feature vectors are generated randomly, and the corresponding labels are provided by massive simulation results performed on the power system frequency response model in Fig. 3:
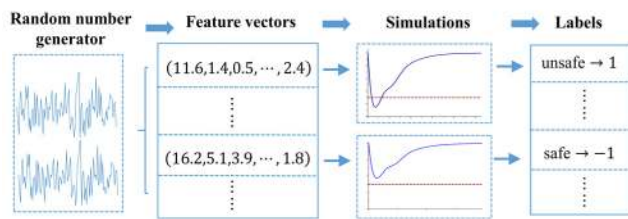

FIGURE 5. Generation of the training dataset.

Later the MLFSC is established with SVM. The main idea is to find a hyperplane represented by parameters $\{w, b\}$ to separate the data with different labels. With the obtained hyperplane, we can get the label of any new feature vector by judging which side of the hyperplane it is located in. With the training dataset $\{\mathbf{x}, \mathbf{y}\}$, the SVM can be trained by solving the following optimization problem [21]:

$$\min_{w,b,\delta} \frac{1}{2}\|w\|^2 + C\sum_{i=1}^{k}\delta_i \quad (24)$$

$$s.t. \ \forall i, \quad y_i[w^T\varphi(x_i) + b] \ge 1 - \delta_i \quad (25)$$

$$\delta_i \ge 0 \quad (26)$$

where $\varphi(\cdot)$ is a mapping from the feature space to a new space, which is of great significance to improve the performance of SVM [21]. δ and C are slack variables and the corresponding cost parameters utilized to penalize feature vectors that are misclassified or too close to the hyperplane.

Assume that λ^* is the optimal Lagrange multipliers associated with (25). It can be obtained by solving the Lagrange dual problem of the original problem (24) – (26) [31]. Then the parameters of the optimal hyperplane can be calculated by:

$$w^* = \sum_{i=1}^{k}\lambda_i^* y_i x_i \quad (27)$$

$$b^* = y_j - \sum_{i=1}^{k} y_i \lambda_i^* (x_i \cdot x_j) \quad (28)$$

where y_j is the label of any point that satisfies $0 < \lambda_j^* < C$.

With the optimal hyperplane, the frequency security constraint (16) can be converted by the trained MLFSC into the following form:

$$\sum_{i=1}^{k}\lambda_i^* y_i K(x_i, x) + b^* + \alpha \le 0 \quad (29)$$

$$x_{(1)} = \Delta P_0 \quad (30)$$

where $x_{(1)}$ represents the first element of x; α is the shift coefficient; $K(x_i, x)$ is the kernel function of the mapping $\varphi(\cdot)$ that satisfies:

$$K(x_i, x) = \varphi(x_i) \cdot \varphi(x) \quad (31)$$

It's clear that the kernel function represents the mapping $\varphi(\cdot)$ implicitly in the form of vector inner products. The polynomial kernel function is a widely used kernel function [21] which is adopted in this paper:

$$K(x_i, x) = (a_0 x_i \cdot x + a_1)^2 \quad (32)$$

where a_0 and a_1 are the polynomial kernel coefficients. It can be seen from (29) and (32) that the original frequency security constraint (16) is converted into a quadratic constraint.

As can be seen, the adoption of polynomial kernel function is a necessary step to enable the general QCQP formulation. Therefore, it is utilized in the SVM model instead of the radial basis function (RBF) [21] or other kernel functions.

C. SUGGEST-AND-IMPROVE METHOD FOR QCQP

The reserve allocation QCQP is nonconvex because y_i in (29) is not ensured to be positive. Consequently, the global optima the problem cannot be solved by the general polynomial-time method for convex QCQP [32]. In this paper, the heuristic SI method [33] is utilized to deal with the nonconvex QCQP of interest.

The main idea of the SI method is to find a candidate which is the lower bound of the original nonconvex QCQP (Suggest procedure) and shift the candidate point to the approximated optima (Improve procedure).

1) SUGGEST PROCEDURE BY SEMIDEFINITE RELAXATION

In the Suggest procedure, semidefinite relaxation (SDR) is utilized to relax the problem and solve it to get the lower bound of the original problem. We first introduce a new variable S and rewrite (29) as:

$$\mathbf{tr}(PS) + q^T x + r \le 0 \quad (33)$$

$$S = xx^T \quad (34)$$

$$P = \sum_{i=1}^{k} \lambda_i^* y_i a_0^2 x_i^T x_i \qquad (35)$$

$$q = \sum_{i=1}^{k} 2\lambda_i^* y_i a_0 a_1 x_i \qquad (36)$$

$$r = \sum_{i=1}^{k} \lambda_i^* y_i a_1^2 + b^* + \alpha \qquad (37)$$

where $\mathbf{tr}()$ represents the trace of a matrix. Note that with the reformulated constraints above, all the objective and constraints are convex except (34). In order to accomplish a convex relaxation, (34) is substituted with:

$$S \geq xx^T \qquad (38)$$

$$S_{(r1)} = \Delta P_0 x^T$$
$$S_{(c1)} = \Delta P_0 x \qquad (39)$$

where $S_{(r1)}$ and $S_{(c1)}$ are the first row and first column of S, respectively.

Due to the convexity, the relaxed problem can be solved easily. Here, the candidate in the Suggest procedure is denoted as the solution $\tilde{x}$.

2) IMPROVE PROCEDURE BY COORDINATE DESCENT

The first step of the Improve procedure is to find a feasible point of the original nonconvex QCQP based on the candidate $\tilde{x}$ obtained in Suggest procedure. We iterate each element $\tilde{x}_{(j)}$ of $\tilde{x}$ to solve the following problem:

$$\min_{t, \tilde{x}_{(j)}} t$$
$$\forall i, \quad f_i(x) \leq t \qquad (40)$$

where $f_i(x) \leq 0$ represents all the constraints of the reserve allocation problem. It is obvious that when $t \leq 0$, the feasible point is obtained and the iteration is terminated. As all elements are fixed except one, the problem (40) can be easily solved by the bisection method proposed in [34].

The second step of Improve procedure is to improve the solution. We iterate each element of the feasible point to solve the nonconvex QCQP until no more improvements can be achieved. Similarly, as only one element is variable during the iteration, the nonconvex QCQP can be solved by the bisection method [34].

The pseudocodes of the SI method are given in Table 1.

IV. CASE STUDIES

In this section, a realistic 12-bus system in Haining, China [35] is utilized to verify the proposed data-driven reserve allocation method, whose topology is illustrated in Fig. 6. The total load of the system is 405 MW. Besides 4 conventional generators, 5104 commercial IACs in the testing system are considered to participate in the frequency regulation. T_{CH} of the four generators are 0.43s, 0.52s, 0.51s and 0.59s, respectively. T_{RH} of the four generators are 4.9s, 4.8s, 5.1s, 4.8s, respectively. Other parameters of the generators are listed in Fig. 6.

TABLE 1. Pseudocodes of the suggest-improve method.

| Suggest procedure |
|---|
| Step1: Relax the QCQP with a new variable S to a convex problem. |
| Step2: **Output** candidate $\tilde{x} \leftarrow$ Solution of the above convex problem |
| **Improve procedure** |
| Step1: Find a feasible point based on $\tilde{x}$: |
| **Input** $\tilde{x}$ |
| **Repeat** |
| **for** $j = 1, 2, \cdots, m+n$ |
| $\tilde{x}_{(j)} \leftarrow$ Solution of (40) |
| **Until** $t \leq 0$ |
| **Output** $\tilde{x}$ |
| Step2: Improve the feasible point: |
| **Input** $\tilde{x}^k \leftarrow \tilde{x}$, e |
| **Repeat** |
| **for** $j = 1, 2, \cdots, m+n$ |
| $\tilde{x}_{(j)}^{k+1} \leftarrow$ Solution of the original QCQP |
| $k \leftarrow k+1$ |
| **Until** $\left\| \tilde{x}^{k+1} - \tilde{x}^k \right\| \leq e$ |
| **Output** $\tilde{x}^{k+1}$ as the approximated optimal solution |
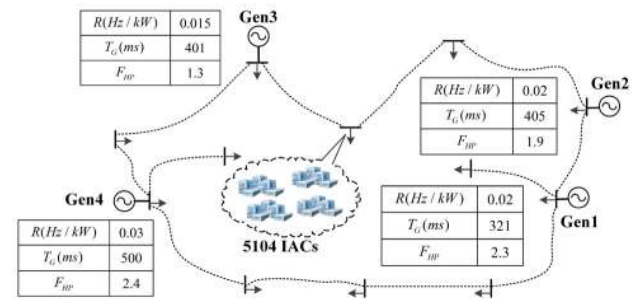
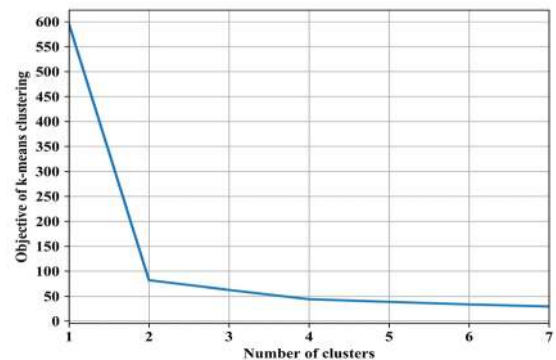**FIGURE 6.** Topology of the testing system.

FIGURE 7. Objective value of the k-means clustering with number of clusters.

A. AGGREGATION OF IACS

Considering the fact that most of the thermal characteristics of the commercial IACs in the same testing area are roughly homogeneous, two parameters named T_c and A are utilized to identify the IACs. The widely utilized elbow method is introduced to determine the cluster number in the k-means algorithm [29], [36], which coordinates the clustering accuracy with the computation efficiency. As indicated in Fig. 7,
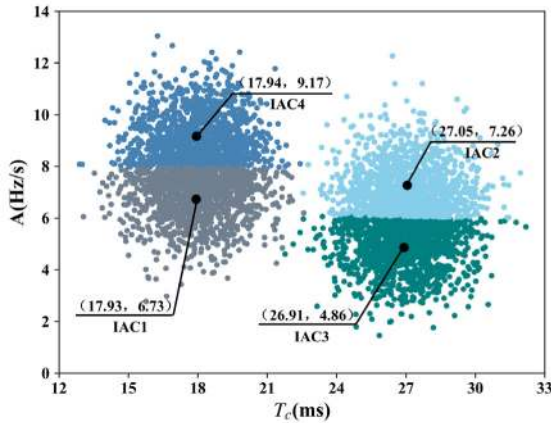
FIGURE 8. IAC aggregation result by k-means clustering.

TABLE 2. Performances of the SI and the gurobi solver.

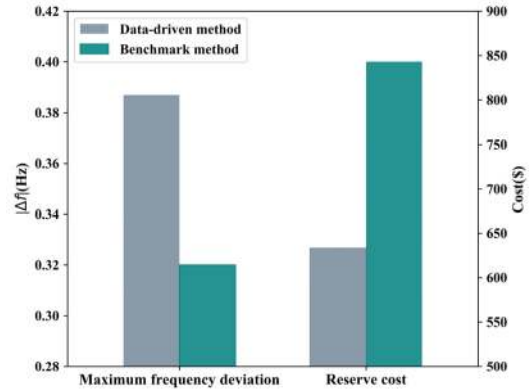|	Obtained objective($)	CPU (ms)
SI method	633.48	78.5
Gurobi solver	633.76	99.2

FIGURE 9. Maximum frequency deviations and the overall costs achieved by the two methods.
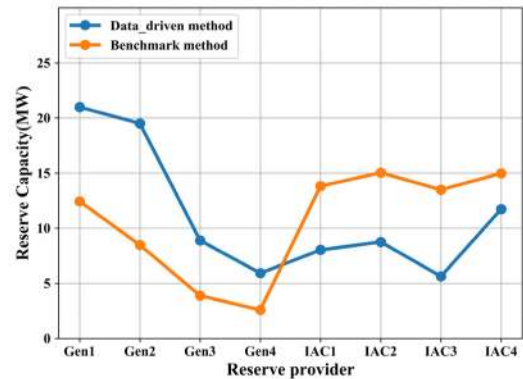

FIGURE 10. Reserve allocation results obtained from the two methods.

the objective value shown in (14) which indicates the error of the clustering, drops with the increase of the number of clusters while the dropping speed gradually slows down. Specifically, the value of the objective has become already quite low since the number of clusters reaches 4. And further significant decrease of the objective value cannot be achieved by adopting more clusters. Therefore, the number of clusters is selected as 4 to ensure the satisfactory accuracy and considerable computation efficiency of the k-means simultaneously. The aggregation result of the IACs with $n = 4$ is presented in Fig. 8, where the black dots represent the four cluster centroids. Note that the parameters of the IACs in Fig. 8 are normalized to [0, 1] for better clustering performance in advance by the following min-max normalization:

$$T_{CN}^i = \frac{T_C^i - \min(\boldsymbol{T}_c)}{\max(\boldsymbol{T}_c) - \min(\boldsymbol{T}_c)} \tag{41}$$

$$A_N^i = \frac{A^i - \min(\boldsymbol{A})}{\max(\boldsymbol{A}) - \min(\boldsymbol{A})} \tag{42}$$

where T_{CN}^i and A_N^i are the normalized T_C^i and A^i, respectively; $\boldsymbol{T}_c$ and $\boldsymbol{A}$ are the sets of T_c and A to be clustered, respectively.

B. RESERVE ALLOCATION RESULTS

In this section, the numerical results of reserve allocation are studied. The maximum allowed frequency deviation $\Delta f_{\max}$ is set as 0.4 Hz. The power imbalance ΔP_0 is 81 MW (20% of the total load). In order to build the training dataset for the MLFSC, 12000 feature vectors are randomly generated subject to Gaussian distributions. The labels of feature vectors are obtained from frequency dynamic simulations. The result from cross-validation [37] indicates that the adoption of polynomial kernel function can achieve higher accuracy (98.91%) than that of RBF (94.17%).

The performance of the utilized SI method is compared with the commercial Gurobi solver in terms of the QCQP presented in Section III. Table 2 illustrates the obtained objectives and CPU time of the two methods. It is indicated that the reserve cost obtained from the SI method are slightly lower

than that of the Gurobi solver. Besides, the CPU calculation time by the SI method is shorter than that by Gurobi solver, which proves that the SI method are more efficient than the latter.

In order to verify the proposed data-driven method better, the numerical comparison with the state-of-the-art method presented in [9] is also implemented. Specifically, the state-of-the-art or the benchmark method linearizes the frequency response of generators and ensures the frequency security constraint by proposing its sufficient condition, which may lead to rather conservative results. The reserve allocation results are illustrated in Fig. 9 and Fig. 10.

As can be seen, the proposed data-driven method is superior to the benchmark method, because the benchmark method is obviously too conservative. Specifically, it is shown in Fig. 9 that the maximum frequency deviation obtained by the benchmark method is more deviated to $\Delta f_{\max}$ than that of the data-driven method. It indicates that the benchmark method tends to overestimate the impact of the

power imbalance on the frequency deviation. The total cost obtained from the data-driven method is only 75% of that of the benchmark method.

It can be seen from Fig. 10 that the proposed data-driven method tends to allocate less reserve to IACs. The reason is that IACs are of faster response speed but higher reserve cost in this testing system, which are prone to be more utilized in conservative schemes. Due to the more precise estimation of frequency response results, the proposed data-driven method enables power system to operate closer to frequency security boundary and thus achieves lower cost. It can be concluded from the comparisons that the reserve allocation suggested by the data-driven method is more optimal than that of the benchmark method.
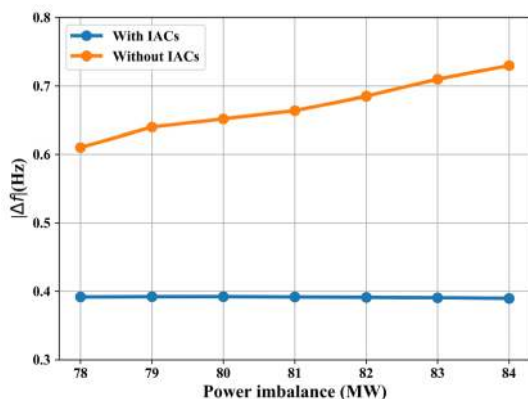

FIGURE 11. Maximum frequency deviation with different power imbalances.

In order to demonstrate the adaptability of the proposed method, the maximum frequency deviations under different power imbalances are shown in Fig. 11. It is clear that with the proposed method, the frequency security constraints can be satisfied quite well. Specifically, the maximum frequency nadir can be kept close to but within the threshold of 0.4 Hz with the increase of ΔP_0. In addition, to illustrate the impact of IACs on the frequency security, the system in which the IACs are excluded from the frequency regulation is also studied. Its maximum frequency deviation values are also shown in Fig. 11. The result shows that there are no solutions satisfying the frequency security constraint in the investigating horizon of ΔP_0. With the reserve completely provided by the conventional generators, the system frequency nadir deviates greatly from Δf_{max} and rises significantly with the increase of ΔP_0.

V. CONCLUSION

In this paper, a data-driven reserve allocation method to deal with implicit frequency security constraint is proposed considering IACs. The equivalent frequency model of aggregated IACs is established and incorporated into power system frequency regulation framework. The reserve allocation is then converted by the MLFSC into a solvable nonconvex QCQP, which is handled by a heuristic SI method. The proposed

method is data-driven as the MLFSC is trained by the labeled dataset of frequency dynamics obtained from the frequency simulations. Compared with the state-of-the-art method, the data-driven method estimates the system frequency dynamics more precisely and obtains lower reserve allocation cost. It can also be concluded that the reserves provided by IACs can significantly improve the frequency security of power system.

Considering the participation of increasing demand-side resources in power system operation, the proposed method is of great significance to improve model-free frequency control and handle big data in smart grids. However, other kinds of flexible resources such as the electric vehicles (EV) are also feasible to participate in power system frequency regulation [38], [39]. In the future work, a more general framework of frequency regulation is to be studied by integrating EVs and other flexible resources. Moreover, advanced machine learning models besides SVM and state-of-the-art optimization algorithms are worth trying in the proposed framework including the MLFSC for better performance.

REFERENCES

[1] A. Atputharajah and T. K. Saha, "Power system blackouts—Literature review," in *Proc. ICIIS*, Dec. 2009, pp. 460–465.

[2] U. Rudez and R. Mihalic, "WAMS-based underfrequency load shedding with short-term frequency prediction," *IEEE Trans. Power Del.*, vol. 31, no. 4, pp. 1912–1920, Aug. 2016.

[3] H. Chvez, R. Baldick, and J. Matevosyan, "The joint adequacy of AGC and primary frequency response in single balancing authority systems," *IEEE Trans. Sustain. Energy*, vol. 6, no. 3, pp. 959–966, Jul. 2015.

[4] Y. G. Rebours, D. S. Kirschen, M. Trotignon, and S. Rossignol, "A survey of frequency and voltage control ancillary services—Part I: Technical features," *IEEE Trans. Power Syst.*, vol. 22, no. 1, pp. 350–357, Feb. 2007.

[5] R. Doherty, A. Mullane, G. Nolan, D. J. Burke, A. Bryson, and M. O'Malley, "An assessment of the impact of wind generation on system frequency control," *IEEE Trans. Power Syst.*, vol. 25, no. 1, pp. 452–460, Feb. 2010.

[6] P. Kundur, N. J. Balu, and M. G. Lauby, *Power System Stability and Control*. New York, NY, USA: McGraw-Hill, 1994.

[7] T. Shekari, F. Aminifar, and M. Sanaye-Pasand, "An analytical adaptive load shedding scheme against severe combinational disturbances," *IEEE Trans. Power Syst.*, vol. 31, no. 5, pp. 4135–4143, Sep. 2016.

[8] Y. Lu, W.-S. Kao, and Y.-T. Chen, "Study of applying load shedding scheme with dynamic D-factor values of various dynamic load models to Taiwan power system," *IEEE Trans. Power Syst.*, vol. 20, no. 4, pp. 1976–1984, Nov. 2005.

[9] C. Liang, P. Wang, X. Han, W. Qin, R. Billinton, and W. Li, "Operational reliability and economics of power systems with considering frequency control processes," *IEEE Trans. Power Syst.*, vol. 32, no. 4, pp. 2570–2580, Jul. 2017.

[10] Y. Wen, W. Li, G. Huang, and X. Liu, "Frequency dynamics constrained unit commitment with battery energy storage," *IEEE Trans. Power Syst.*, vol. 31, no. 6, pp. 5115–5125, Nov. 2016.

[11] Y.-Q. Bao, Y. Li, B. Wang, M. Hu, and Y. Zhou, "Day-ahead scheduling considering demand response as a frequency control resource," *Energies*, vol. 10, no. 1, p. 82, Jan. 2017.

[12] D. Xie, H. Hui, Y. Ding, and Z. Lin, "Operating reserve capacity evaluation of aggregated heterogeneous TCLs with price signals," *Appl. Energy*, vol. 216, pp. 338–347, Apr. 2018.

[13] F. Ruelens, B. J. Claessens, S. Vandael, B. De Schutter, R. Babuška, and R. Belmans, "Residential demand response of thermostatically controlled loads using batch reinforcement learning," *IEEE Trans. Smart Grid*, vol. 8, no. 5, pp. 2149–2159, Sep. 2017.

[14] M. Isaac and D. P. van Vuuren, "Modeling global residential sector energy demand for heating and air conditioning in the context of climate change," *Energy Policy*, vol. 37, no. 2, pp. 507–521, Feb. 2009.

[15] BusinessLine. (2017). *AC Makers Betting on Consumers' Shift to Inverter Models*. [Online]. Available: http://www.thehindubusinessline.com.

[16] J. C. Hwang, "Assessment of air condition load management by load survey in Taipower," *IEEE Trans. Power Syst.*, vol. 16, no. 4, pp. 910–915, Nov. 2001.

[17] Bijli Bachao. (2017). *What is Inverter Technology AC*. [Online]. Available: https://www.bijlibachao.com.

[18] M. Song, C. Gao, H. Yan, and J. Yang, "Thermal battery modeling of inverter air conditioning for demand response," *IEEE Trans. Smart Grid*, vol. 9, no. 6, pp. 5522–5534, Nov. 2018.

[19] H. Hui, Y. Ding, and M. Zheng, "Equivalent modeling of inverter air conditioners for providing frequency regulation service," *IEEE Trans. Ind Electron.*, vol. 66, no. 2, pp. 1413–1423, Feb. 2019.

[20] Y. Ding, Y. Song, H. Hui, and C. Shao, *Integration of Air Conditioning and Heating Into Modern Power Systems*. Singapore: Springer, 2019.

[21] B. Schlkopf and A. J. Smola, *Learning With Kernels: Support Vector Machines, Regularization, Optimization, and Beyond*. Cambridge, MA, USA: MIT Press, 2001.

[22] N. Huang, H. Chen, G. Cai, L. Fang, and Y. Wang, "Mechanical fault diagnosis of high voltage circuit breakers based on variational mode decomposition and multi-layer classifier," *Sensors*, vol. 16, no. 11, p. 1887, 2016.

[23] P. P. K. Chan, W.-C. Chen, W. W. Y. Ng, and D. S. Yeung, "Multiple classifier system for short term load forecast of microgrid," in *Proc. ICMLC*, Guilin, China, Jul. 2011, pp. 1268–1273.

[24] O. P. Mahela, A. G. Shaik, and N. Gupta, "A critical review of detection and classification of power quality events," *Renew. Sustain. Energy Rev.*, vol. 41, pp. 495–505, Jan. 2015.

[25] Z.-Q. Luo, W.-K. Ma, A. M.-C. So, Y. Ye, and S. Zhang, "Semidefinite relaxation of quadratic optimization problems," *IEEE Signal Process. Mag.*, vol. 27, no. 3, pp. 20–34, May 2010.

[26] S. Ihara and F. C. Schweppe, "Physically based modeling of cold load pickup," *IEEE Trans. Power App Syst.*, vol. PAS-100, no. 9, pp. 4142–4150, Sep. 1981.

[27] China Household Appliance Standard and Technology Industry Alliance. (2016). *Midea and State Grid Jiangsu Corporation Reached Strategic Cooperation, Piloting Internet + Smart Power Consuming Project*. [Online]. Available: http://www.chasa.com.cn/2016/0826/208.shtml

[28] IFENG. (2017). *Raising the Curtain of the Popularization of Smart Air Conditioners: Haier Became the Exporter of Innovative Models*. [Online]. Available: http://home.ifeng.com/a/20170216/44544226_0.shtml

[29] J. A. Hartigan and M. A. Wong, "Algorithm AS 136: A K-means clustering algorithm," *Appl. Statist.*, vol. 28, no. 1, pp. 100–108, 1979.

[30] N. Ruiz, I. Cobelo, and J. Oyarzabal, "A direct load control model for virtual power plant management," *IEEE Trans. Power Syst.*, vol. 24, no. 2, pp. 959–966, May 2009.

[31] S. Boyd and L. Vandenberghe, *Convex Optimization*. Cambridge, U.K.: Cambridge Univ. Press, 2004.

[32] R. Misener and C. A. Floudas, "GloMIQO: Global mixed-integer quadratic optimizer," *J. Global Optim.*, vol. 57, no. 1, pp. 3–50, Sep. 2013.

[33] J. Park and S. Boyd, "General heuristics for nonconvex quadratically constrained quadratic programming," Mar. 2017, *arXiv:1703.07870*. [Online]. Available: https://arxiv.org/abs/1703.07870

[34] J. Park, "Approximation techniques for mixed-integer quadratic programs," Ph.D. dissertation, Dept. Math., Univ. Stanford, Palo Alto, CA, USA, 2017.

[35] W. Wang, L. Yang, L. Wang, P. Zhang, J. Huang, and K. Wang, "Optimal dispatch of integrated electricity-heat energy system considering heat storage characteristics of heating network," *Autom. Electr. Power Syst.*, vol. 21, pp. 45–52, Nov. 2018.

[36] Y. Guo, H. Gao, and Q. Wu, "A combined reliability model of VSC-HVDC connected offshore wind farms considering wind speed correlation," *IEEE Trans. Sustain. Energy*, vol. 8, no. 4, pp. 1637–1646, Oct. 2017.

[37] I. Goodfellow, Y. Bengio, A. Courville, and F. Bach, *Deep Learning*. London, U.K.: MIT Press, 2016.

[38] H. Hao, B. M. Sanandaji, K. Poolla, and T. L. Vincent, "Frequency regulation from flexible loads: Potential, economics, and implementation," in *Proc. ACC*, Portland, OR, USA, Jun. 2014, pp. 65–72.

[39] S. Izadkhast, P. Garcia-Gonzalez, and P. Frías, "An aggregate model of plug-in electric vehicles for primary frequency control," *IEEE Trans. Power Syst.*, vol. 30, no. 3, pp. 1475–1482, May 2015.

XINRAN ZHUANG received the B.Eng. degree in electrical engineering from Zhejiang University, Hangzhou, China, in 2017, where he is currently pursuing the M.S. degree in electrical engineering. His research interests include smart grid and machine learning in power systems.

CHENGJIN YE received the B.E. and Ph.D. degrees in electrical engineering from Zhejiang University, China, in 2010 and 2015, respectively. He was as a Distribution System Engineer with the Economics Research Institute of State Grid Zhejiang Electric Power Company Ltd., from 2015 to 2017. Since June 2017, he has been with the Smart Grid Operation and Optimization Laboratory (SGOOL) and a Postdoc Researcher with the College of Electrical Engineering, Zhejiang University. His research interests include data-driven power system planning and operation, short-circuit current limitation, and grid resilience enhancement considering extreme events.

YI DING received the B.Eng. degree in electrical engineering from Shanghai Jiaotong University, China, and the Ph.D. degree in electrical engineering from Nanyang Technological University (NTU), Singapore. He was an Associate Professor with the Department of Electrical Engineering, Technical University of Denmark, Denmark. He also held research and teaching positions at University of Alberta, Canada, and NTU. He is currently a Professor with the College of Electrical Engineering, Zhejiang University (ZJU), China. His research interests include power system planning and reliability evaluation, smart grid, and complex system risk assessment.

HONGXUN HUI received the bachelor's degree in electrical engineering from Zhejiang University, Hangzhou, China, in 2015, where he is currently pursuing the Ph.D. degree in electrical engineering. He was elected in the first batch of the Academic Rising Star Program in Zhejiang University, in 2018. His research interests include modeling and optimal control of demand side resources in smart grid, the electricity market considering demand response, and the uncertainty analysis brought by flexible loads and renewable energies.

BO ZOU received the Ph.D. degree in electrical engineering from Zhejiang University, Hangzhou, China, in 2016. He is currently a Senior Engineer with the Economics Research Institute of State Grid Zhejiang Electric Power Company Ltd., Hangzhou. His research interests include smart grids and power system planning.

• • •